Three Novel Isomeric Zinc Metal−Organic Frameworks from a Tetracarboxylate Linker

Yun-Xia Hu,[†,‡] Hai-Bo Ma,[†] Bo Zheng,[†] Wen-Wei Zhang,*,[†] Shengchang Xiang,[∥] Lu Zhai,[†,§] Li-Feng Wang,[†,§] Banglin Chen,[∥] Xiao-Ming Ren,[§] and Junfeng Bai*,[†]

[†]State Key Laboratory of Coordination Chemistry and Institute of Theoretical and Computational Chemistry, Key Laboratory of Mesoscopic Chemistry of MOE, School of Chemistry and Chemical Engineering, Nanjing University, Nanjing 210093, China

[‡]Xinjiang Laboratory of Phase Transitions and Microstructures in Condensed Matters, College of Chemistry and Biological Sciences, Yili Normal University, Yili, Xinjiang 835000, China

[§]Department of Applied Chemistry, College of Science, Nanjing University of Technology, Nanjing 210009, China

[∥]Department of Chemistry, University of Texas at San Antonio, San Antonio, Texas 78249-0698, United States

Ⓢ *Supporting Information*

ABSTRACT: Three porous supramolecular isomers (**IZE-1**, **IZE-2**, and **IZE-3**) with the same framework component [$Zn_2(EBTC)(H_2O)_2$] (EBTC = 1,1′-ethynebenzene-3,3′,5,5′-tetracarboxylate) were successfully constructed by finely tuning the reaction condition. Although both **IZE-1** and **IZE-2** are constructed from the linear EBTC subunits and one kind of regular [$Zn_2(CO_2)_4$] paddlewheels, their frameworks exhibit two different (3,4)-c net of **fof** (sqc1575) and sqc1572, respectively, resulting in cavities with different size and shape. However, as for isomer **IZE-3**, the EBTC ligands are bent and one-half of the [$Zn_2(CO_2)_4$] paddlewheels are distorted, leading to a novel (3,4,4)-c **hyx** net with point symbol $(6.7^2)_4(6^2.8^2.10^2)(7^2.8^2.11^2)$ and vertex symbol $(6.7.7)_4(7_2.7_2.8.8.12.12)(6.6.8.8.10_2.10_2)$. Quantum chemical calculations by DFT indicate that the three isomers have very close thermodynamic stabilities, which may explain that subtle condition change leads to variation of the frameworks. Further theoretical semiempirical investigation on the interactions between solvent molecules and compounds shows different hydrogen binding patterns in good agreement with the experimental observations. Furthermore, they exhibit good solid-state luminescence properties with long lifetime.
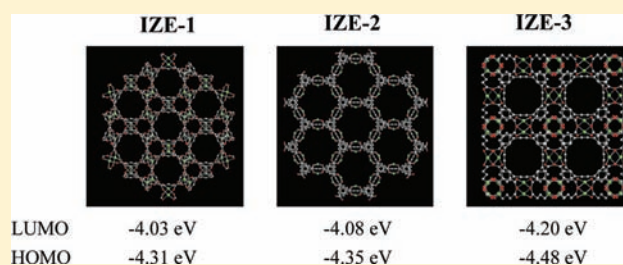
INTRODUCTION

Very recently, porous metal−organic frameworks (MOFs) became of higher interest in modern materials science since they may offer great promise in applications such as gas storage, separations, catalysis, sensors, electronics, and drug delivery.[1] In particular, MOFs possess flexible and tunable pores, making themselves exceed other porous compounds.[1b,c] However, structural uncertainty and diversity are the main intrinsic problems for crystallization and construction during self-assembly,[2] since the porous network formation is sensitive to many aspects, such as the ligand structure,[3] the coordination geometry preferred by the metal,[4] the method of crystallization,[5] reaction temperature,[6] the solvent system,[7] pH value,[6b,8] and the metal-to-ligand ratio,[9] etc. Meanwhile, supramolecular isomerism was occasionally reported during the construction of MOFs starting from the same reactants,[10,11] and now it is attracting more and more interest since it affords a good opportunity for developing novel materials and makes a better understanding of the structure−property relationships of coordination polymers.[2] However, considering the wide occurrence of structural and compositional uncertainty and diversity during self-assembly, rational realization of a supra-

molecular isomerism system, even the simplest one, would be extremely difficult up to date.[2]

Nowadays, paddlewheel-based porous MOFs with $M_2(CO_2)_4$ (M = Cu, Zn) inorganic secondary building units (SBUs) have been widely constructed by organic linkers with multiple carboxylate groups including dicarboxylate,[12] tricarboxylate,[10i,13] tetracarboxylate,[12d,14] hexacarboxylate,[15] and so on. Recently, in our and some other groups, tetracarboxylate ligand EBTC (EBTC = 1,1′-ethynebenzene-3,3′,5,5′-tetracarboxylate, Scheme 1) has been designed to construct dicopper paddlewheel porous MOFs with nbo-type topology, exhibiting excellent adsorption properties.[10m,16] However, while constructing dizinc paddlewheel porous MOFs based on it, some interesting results were found. Three framework isomers[11b] of dizinc paddlewheel porous MOFs originated from differences in orientation or conformation were obtained, which were sensitive to the synthetic conditions. Herein we report the controllable isomerization of such three porous frameworks formed under different synthetic conditions.

Scheme 1. Illustration for the Molecular Structure of H₄EBTC
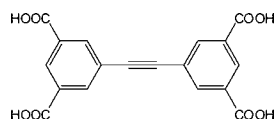
■ EXPERIMENTAL SECTION

Materials and General Methods. *N,N*-Dimethylformamide (DMF) and dimethylsulfoxide (DMSO) were dried and distilled according to standard procedures. All other starting materials and solvents were obtained from commercial sources and used without further purification. 1,1′-Ethynebenzene-3,3′,5,5′-tetracarboxylic acid (H₄EBTC) was prepared according to the previously published methods.[17] Elemental analyses (C, H, and N) were carried out on a Perkin-Elmer 240 analyzer. The IR spectra were obtained on a VECTOR TM 22 spectrometer with KBr pellets in the 4000−400 cm⁻¹ region. TGA-DTA diagrams were recorded by a CA Instruments DTA-TGA 2960 type simultaneous analyzer heating from 293 to 1073 K in nitrogen atmosphere at a rate of 20 K/min. Powder X-ray diffraction (PXRD) data were recorded on a Shimadzu XRD-6000 diffractometer with Cu Kα. (λ = 1.540 56 Å) radiation at room temperature with a scan speed of 5°/min and a step size of 0.02 in 2θ. Luminescence spectra for the solid samples were recorded with a Hitachi 850 fluorescence spectrophotometer. The photoluminescence lifetime was measured with an Edinburgh Instruments FLS920P fluorescence spectrometer. Software TOPOS 4.0[18a] was used to compute the topological description.

Synthesis of the Compounds. *Synthesis of [Zn₂(EBTC)-(H₂O)₂]·5.5H₂O·2.5DMF (IZE-1).* The reactants of H4EBTC (5.0 mg, 0.014 mmol) and Zn(NO₃)₂·6H₂O (15.0 mg, 0.05 mmol) were ultrasonically dissolved in anhydrous DMF (0.4 mL) in an 8 mL glass vial, then HNO₃ (0.060 mL, 1.0 M in DMF) was added, and the mixture was sealed and heated to 85 °C for 10 h. After cooling to room temperature, colorless block-shaped crystals were grown and isolated by filtration (8.4 mg, 79.2% based on H₄EBTC). Anal. (%) Calcd for **IZE-1**: C 39.20, H 4.39, N 3.81. Found: C 38.79, H 4.49, N 3.82. IR (KBr pellet, cm⁻¹): 3424−2919 (br, m), 1629 (vs), 1579 (vs), 1430 (vs), 1380 (vs), 1105 (w), 1020 (m), 952 (w), 777 (s), 723 (m), 543 (w).

Synthesis of [Zn₂(EBTC)(H₂O)₂]·10.5H₂O·0.5DMF·0.5DMSO (IZE-2). The reactants of H₄EBTC (5.0 mg, 0.014 mmol), Zn-(NO₃)₂·6H₂O (15.0 mg, 0.05 mmol), and 5-aminoisophthalic acid (AIP) (2.5 mg, 0.014 mmol) were ultrasonically dissolved in a freshly distilled solvent of DMF (0.2 mL) and DMSO (0.2 mL) in an 8 mL glass vial. After the mixture was sealed and heated at 85 °C for 10 h, colorless cuboid-shaped crystals were achieved (10.2 mg, 92.5% based on H₄EBTC). Anal. (%) Calcd for **IZE-2**: C 31.49, H 4.83, N 0.90. Found: C 31.88, H 4.42, N 1.02. IR (KBr pellet, cm⁻¹): 3357−2917 (br, m), 1631 (vs), 1585 (vs), 1376 (vs), 1103 (w), 1020 (s), 952 (m), 906 (w), 777 (s), 727 (m), 673 (m), 620 (w), 511 (w).

Synthesis of [Zn₂(EBTC)(H₂O)₂]·1.5H₂O·2DMF (IZE-3). In a similar way, add 1,3-bi-4-pyridylpropane (BPP) (2.7 mg, 0.014 mmol) to the mixture composed of the same amount of the ligand, the zinc salt, the solvent, and the nitric acid as for the preparation of **IZE-1**, and after the same reaction time at 85 °C, colorless wedge-shaped isomer **IZE-3** was formed (8.5 mg, 87.6% based on H₄EBTC). Anal. (%) Calcd for **IZE-3**: C 41.76, H 3.94, N 4.06. Found: C 42.47, H 3.52, N 3.82. IR (KBr pellet, cm⁻¹): 3411−3073 (br, m), 2929 (m), 1656 (vs), 1622 (vs),1569 (s), 1431 (vs), 1228 (w), 1099 (m), 916 (w), 777 (s), 723 (s), 685 (w), 534 (w).

X-ray Crystallography. X-ray crystallographic intensity data were measured on a Bruker Smart Apex II CCD diffractometer at room temperature using graphite monochromated Mo Kα radiation (λ = 0.710 73 Å). Data reduction was made with the Bruker Saint program. The structures were solved by direct methods and subsequent difference Fourier syntheses, and refined using the SHELXTL software package. The H atoms on the ligands were placed in idealized

positions and refined using a riding model. The H atoms of the coordinated H₂O molecules could not be located, but are included in the formula. The unit cell includes a large region of disordered solvent molecules, which could not be modeled as discrete atomic sites. We employed PLATON/SQUEEZE[18b,c] to calculate the diffraction contribution of the solvent molecules and, thereby, to produce a set of solvent-free diffraction intensities. Crystal data and structure refinement information for the three complexes are listed in Table

Table 1. Crystal Data and Structure Refinement Information for IZE-1, IZE-2, and IZE-3

complex	IZE-1	IZE-2	IZE-3
empirical formula	C₉H₃O₅Zn	C₉H₃O₅Zn	C₉H₃O₅Zn
fw	256.50	256.50	256.50
T (K)	293	293	291
wavelength (Å)	0.710 73	0.710 73	0.710 73
cryst syst	trigonal	trigonal	tetragonal
space group	$R\bar{3}m$	$R\bar{3}m$	$P4(2)/nnm$
a (Å)	19.0504(8)	23.8339(9)	17.2089(12)
b (Å)	19.0504(8)	23.8339(9)	17.2089(12)
c (Å)	32.392(3)	20.2720(17)	28.523(4)
α (deg)	90	90	90
β (deg)	90	90	90
γ (deg)	120	120	90
V (Å³)	10 180.8(10)	9972.8(10)	8446.9(15)
Z	18	18	16
D_{calcd} (g cm³)^a	0.753	0.769	0.813
μ (mm⁻¹)	1.083	1.106	1.161
$F(000)$	2322	2322	2064
θ range (deg)	2.14−28.21	2.80−25.35	1.67−26.00
GOF on F^2	1.096	1.016	0.982
R1, wR2 ($I > 2\sigma(I)$)	0.0595, 0.1823	0.0966, 0.2670	0.0492, 0.1292
R1, wR2 (all data)	0.0750, 0.2013	0.1193, 0.2827	0.0653, 0.1340

^{a}The values are calculated without guest molecules.

1. The main bond lengths and angles are summarized in Tables S1, S2, and S3 (Supporting Information), respectively. Crystallographic data of them have been deposited with the CCDC as deposition Nos. 763157−763159. These data can be obtained free of charge from the Cambridge Crystallographic Data Centre via www.ccdc.cam.ac.uk/data_request/cif.

■ RESULTS AND DISCUSSION

Syntheses and Crystal Structures. Using a rectangular and relatively rigid tetracarboxylate EBTC as ligand, and Zn(NO₃)₂·6H₂O as metallic salt, three porous isomers of [Zn₂(EBTC)(H₂O)₂]ₙ with different frameworks were prepared under different synthetic medium by solvothermal reactions (Figure 1, Figure S1). By single-crystal X-ray diffraction studies, elemental analysis, and thermal gravimetric analysis, **IZE-1**, **IZE-2**, and **IZE-3** were formulated as [Zn₂(EBTC)(H₂O)₂]·5.5H₂O·2.5DMF, [Zn₂(EBTC)-(H₂O)₂]·10.5H₂O·0.5DMF·0.5DMSO, and [Zn₂(EBTC)-(H₂O)₂]·1.5H₂O·2DMF, respectively. It is evident that the reaction medium has a great effect on isomerism since all other reaction conditions are the same, such as the concentration and stoichiometric ratio of the reactants, reaction temperature and time, and the method of crystallization, etc. As a result, even a minor change in a synthesis condition would lead the eventual compound to a quite different structure since the three isomers have similar relative stabilities, which will be discussed in detail below.
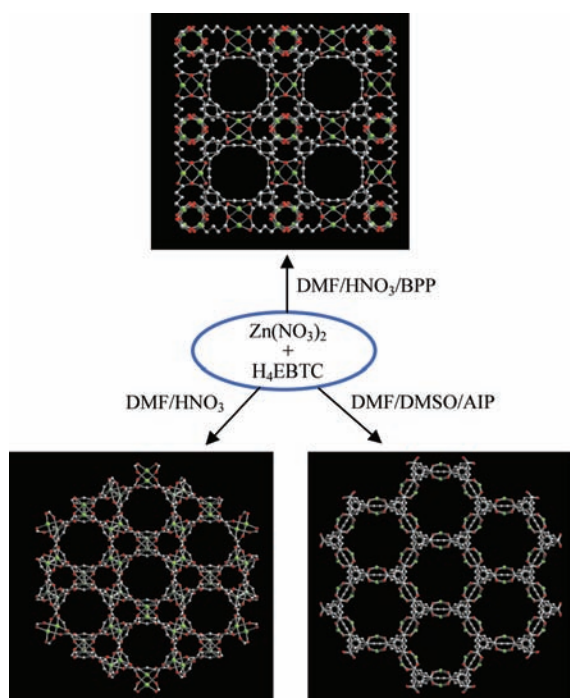
Figure 1. Reaction scheme and drawings of crystal structures of coordination isomeric assemblies **IZE-1** (left), **IZE-2** (right), and **IZE-3** (upper) seen from the *c* direction (AIP = 5-aminoisophthalic acid; BPP = 1,3-bi-4-pyridylpropane). All the H atoms and the coordinated O atoms of water have been omitted for clarity. Color scheme: Zn, green; O, red; C, gray.

X-ray crystallographic analysis reveals that the three complexes are porous isomeric coordination polymers with the same skeleton component $[Zn_2(EBTC)(H_2O)_2]$, in which dizinc paddlewheel SBUs with different motifs are generated. Their structural differences can be clearly discerned from their packing views along the *c*-axes as shown in Figure 1.

Single crystal X-ray crystallographic studies indicates that both **IZE-1** and **IZE-2** crystallize in the $R\overline{3}m$ space group with one-half zinc atom, one-fourth EBTC ligand, and one-half water molecule for the framework in the asymmetric unit. In **IZE-1**, besides a coordinated terminal water molecule in the axial position, each Zn atom coordinates to four carboxylate oxygen atoms from four different EBTC ligands to form one kind of regular $[Zn_2(CO_2)_4]$ paddlewheels which are shown in Figure S2a. The Zn−O−O−Zn torsion angle is 2.302°. The ethynylene bond of the coordinated EBTC ligand almost keeps its linearity (the C5D−C5−C4 angle is 179.8(8)°, symmetry code: D = $^2/_3 + x − y$, $^4/_3 − y$, $^7/_3 − z$) with a bond length of 1.147(10) Å, the two phenyl rings in it are coplanar by symmetry, and the coordinated carboxylate groups are almost coplanar with the phenyls by a small dihedral angle of 4.313°. Likewise, each EBTC ligand is linked to four dizinc paddlewheels via the bridging carboxylate groups. In this kind of 3D framework formed by the interconnected zinc paddlewheels and EBTC ligands, there exists one-dimensional pore along the *c* axis, where its pore window is constructed from three phenyls and three $[Zn_2(CO_2)_4]$ paddlewheels from the same end of EBTC ligand, and the lower paddlewheels directly lie beneath the upper phenyls layer by layer (Figure S2b and Figure 1). Moreover, along the *a* and *b* axis, there also exists a one-dimensional cavity with its pore window constructed from two EBTC ligands, one phenyl group, and

three inorganic paddlewheel SBUs (Figure S2c,d). For insight into its framework, it consists of two different types of open cages which are alternately stacked with each other (Figure 2a):
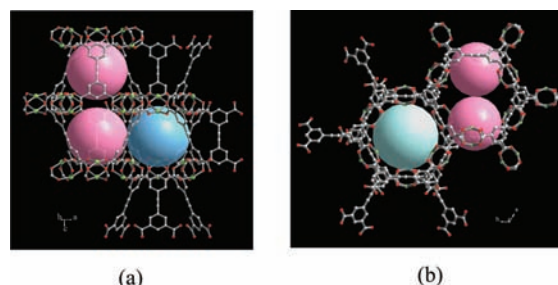

Figure 2. (a) X-ray single crystal structure of **IZE-1** showing two types of cages: small one of about 7.4 Å in diameter (blue sphere) and large elliptical one of about 17.0 × 10.6 Å (pink sphere). (b) X-ray single crystal structure of **IZE-2** showing two types of cages: small one of about 7.4 Å in diameter (blue sphere) and large irregular elongated one of about 15.2 × 11.6 Å^2 (pink sphere). The presented dimension data have subtracted the van der Waals radii of the atoms at opposite sites of the cage. Color scheme: Zn, green; O, red; C, gray. Hydrogen atoms and guest molecules are omitted for clarity.

the small cage is about 7.4 Å in diameter encapsulated by 6 paddlewheel $Zn_2(CO_2)_4$ clusters and 12 EBTC ligands, and the large elliptical cavity is about 17.0 × 10.6 Å^2 surrounded by 12 $Zn_2(CO_2)_4$ inorganic SBUs and 6 EBTC organic SBUs (the van der Waals radii of the atoms at opposite sites of the cage have been subtracted). **IZE-1** possesses very large solvent accessible pore volume which reaches 69.2% of the unit cell volume as calculated by PLATON/SOLV[18b] due to the elongated EBTC ligand.

Just like MOF-505, $[Cu_2(EBTC)(H_2O)_2]$, and some other complexes,[9−13] two kinds of SBUs are contributed to the construction of **IZE-1**. When considering both the dinuclear $Zn_2(CO_2)_4$ SBU and the EBTC ligand as planar 4-c nodes, **IZE-1** would adopt the cubic 4-c **nbo** net. However, this initial description often generates confusion. A better description could be obtained by the following: the $Zn_2(CO_2)_4$ paddlewheel can be served as planar 4-c node which is defined by the carboxylate carbon atoms, and the organic EBTC linker can be considered as two 3-c nodes centered between two phenyl rings (Figure S2e), leading to two different (3,4)-c nets.[10m,19a,b] In this view, **IZE-1** is observed as (3,4)-c **fof** net[19c] (alternative name **sqc**1575),[19a,b,d] with point symbol of $(6.8^2)_2(6^2.8^2.10^2)$ and vertex symbol of $(6.8_2.8_2)$-$(6.6.8_2.8_2.10_2.10_2)$ (Figure S2f).[19e]

The case of isomer **IZE-2** is similar to that of **IZE-1**. In isomer **IZE-2**, the main skeleton of EBTC ligand also does not distort upon assembly with zinc ions, in which the ethynylene bond length is 1.145 (4) Å, the C6D−C6−C3 angle containing the ethynylene group is 179.994(1)° (symmetry code: D = $^1/_3 − x$, $^4/_3 − y$, $^2/_3 − z$), and the dihedral angle of the two phenyl rings in EBTC is zero. The carboxylate groups of EBTC ligand coordinate to Zn^{2+} to form a kind of relative regular $Zn_2(CO_2)_4$ paddlewheels with the Zn−O−O−Zn torsion angle of 3.099° (Figure S3a), a little larger than that in **IZE-1**. The dihedral angle of the coordinated oxygens with the adjacent phenyl is about 9.86°, which is also a little larger than that in **IZE-1**. As illustrated in Figure 1, **IZE-2** also has one-dimensional pore along the *c* axis, where its pore window is formed by three EBTC ligands and three $Zn_2(CO_2)_4$ paddlewheels from the
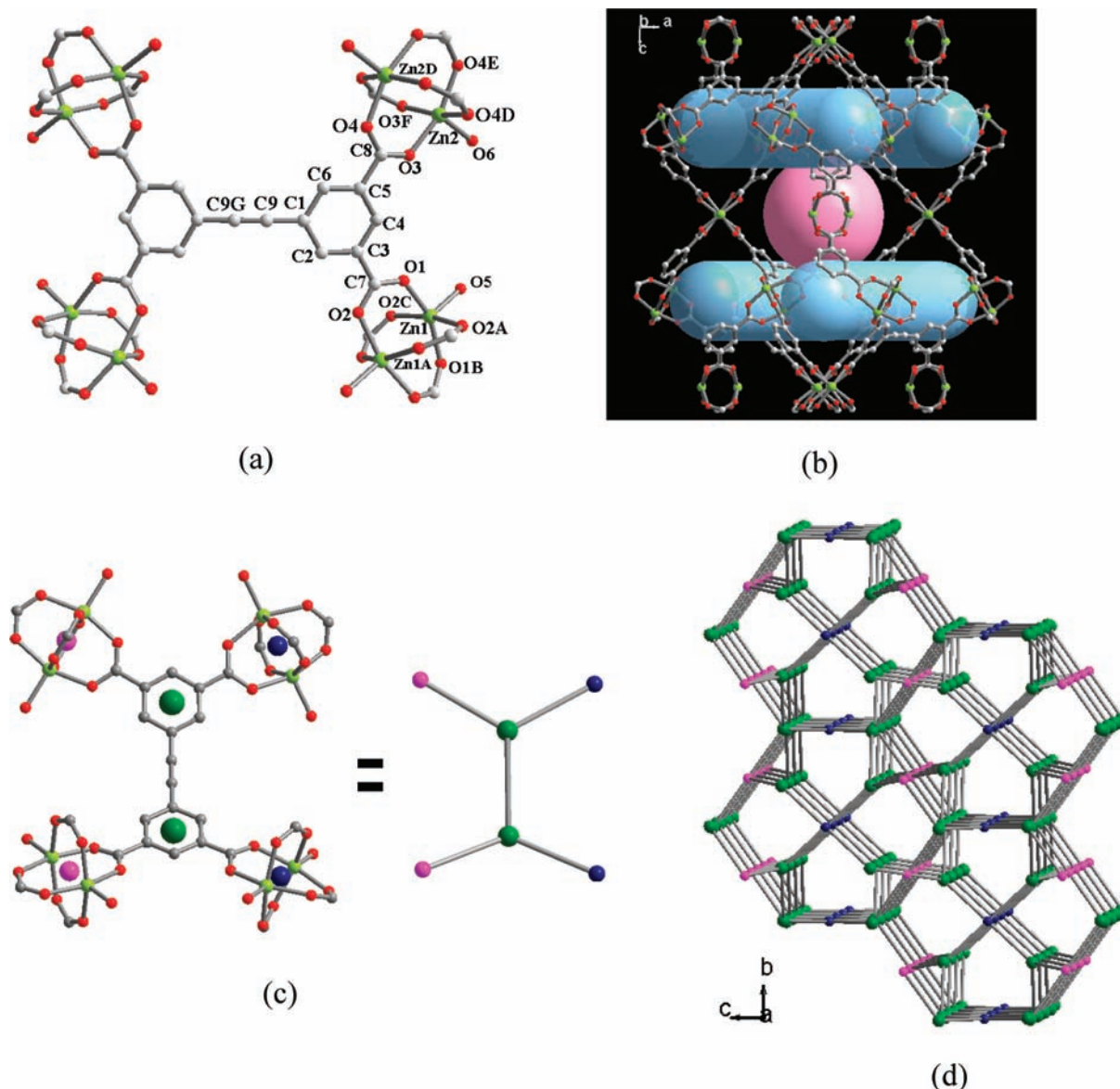
Figure 3. X-ray crystal structure of **IZE-3**: (a) The asymmetric unit and the coordination modes of zinc and EBTC ligand. Hydrogen atoms are omitted for clarity. Symmetry codes: A = $^1/_2 - x$, $^1/_2 - y$, z; B = x, $^1/_2 - y$, $^1/_2 - z$; C = $^1/_2 - x$, y, $^1/_2 - z$; D = y, x, $1 - z$; E = $-x$, $-y$, $1 - z$; F = $-y$, $-x$, z; G = $^1/_2 + y$, $-^1/_2 + x$, z. Color scheme: Zn, green; C, gray; O, red. (b) The open cage (pink sphere) surrounded by four one-dimensional channels (blue portion). (c) Simplification of the organic EBTC linker (two 3-c node, green balls) and the inorganic $Zn_2(CO_2)_4(H_2O)_2$ paddlewheels (two types of 4-c node, pink balls indicate regular paddlewheels and blue balls indicate distorted paddlewheels). (d) Topological view of **IZE-3** with the (3,4,4)-c **hyx** net.

opposite ends of the tetracarboxylate ligand, during which the upper ligands and the lower paddlewheels are arranged layer by layer (Figure S3b and Figure 1). Furthermore, there also exists one-dimensional pore along the a and b axis, with its pore window constructing from one EBTC ligand, two phenyl groups, and three $Zn_2(CO_2)_4$ SBUs (Figure S3c,d). Further investigation indicates that two different types of open cages are alternately presented in its framework (Figure 2b). The small cage is encircled by 6 paddlewheel $Zn_2(CO_2)_4$ clusters and 12 EBTC ligands with 7.4 Å in diameter, and the large irregular elongated cage is surrounded by 12 inorganic SBUs and 6 organic SBUs with the dimension of 15.2 × 11.6 Å² (the van der Waals radii of the atoms at opposite sites of the cage have been subtracted). Its total solvent-accessible pore volume from single crystal structure is 68.0% calculated from PLATON/SOLV,[18b] a little smaller than that of **IZE-1**. Just like the case in

IZE-1, if the linker were to be considered as one 4-c branching point linked to the 4-c paddlewheel vertex, the underlying net of **IZE-2** would also be the cubic 4-c **nbo** net, where the ligand orientation difference between **IZE-2** and **IZE-1** is not represented in the vertex symbol.[10m] But, if the ligands of EBTC in **IZE-2** were also to be considered as two 3-c vertices linked to the 4-c inorganic paddlewheel vertex, then its framework would be the (3,4)-c **sqc1572** net,[10m,19a−d,20] with point symbol of $(7^3)_2(7^4.10^2)$ and vertex symbol of $(7.7.7_2)$ $(7.7.7_2.7_2.10_2.10_2)$[19e] (Figure S3e).

IZE-3 crystallizes in the space group $P4(2)/nnm$ consisting of two Zn(II) centers, one-half EBTC ligand, and two water molecules for the framework in the asymmetric unit (Figure 3a). Unlike crystal **IZE-1** and **IZE-2**, the ethynylene bond of the EBTC ligand in crystal **IZE-3** deviates from its linearity with the C9G−C9−C1 angle of 173.82(19)° (symmetry code:

G = $^1/_2 + y, -^1/_2 + x, z$), which results to a longer bond length of 1.197(5) Å compared to that in **IZE-1** and **IZE-2**, and the two phenyl rings in it are not in the same plane any more with a dihedral angle of 22.23°. In the meanwhile, the coordinated oxygens are deflected from the phenyl plane with a dihedral angle of about 10.96° and 14.09°, respectively, which are much larger than those in isomer **IZE-1** and **IZE-2**. As shown in Figure 3a, besides coordinating to one oxygen atom in the axial position coming from a water molecule, Zn1 atoms coordinate to four carboxylate oxygen atoms in the horizontal plane coming from four different EBTC ligands to construct a kind of distorted $[Zn_2(CO_2)_4]$ paddlewheels with a Zn−O−O−Zn torsion angle of 19.767°, while Zn2 atoms coordinate to four carboxylate oxygen atoms from four different EBTC ligands to assemble a kind of relatively regular $[Zn_2(CO_2)_4]$ paddlewheels with a Zn−O−O−Zn torsion angle of 1.035°. As a result, every EBTC connects two distorted and two regular dizinc paddlewheels, which are *cis* to each other. There also exists one-dimensional pore along the *c* axis (Figure 1), where its pore window is formed by two EBTC ligands and two $Zn_2(CO_2)_4$ paddlewheels from the opposite ends of the tetracarboxylate ligand, and the upper and the lower ligands are staggered arranged layer by layer (Figure S4a). Besides above, two other kinds of one-dimensional pores exist along the *a* and *b* axis (Figure S4b,c). Furthermore, it is noteworthy that not only open cages but also multiple one-dimensional tunnels are formed by the two kinds of different zinc paddlewheels interconnected with EBTC ligands in this 3D framework. As shown in Figures 3b and S4d,e, every open cage constructed from four regular and four distorted $Zn_2(CO_2)_4$ clusters and four EBTC ligands is surrounded by four one-dimensional channels arranged at two different directions, with a diameter of 7.6 Å ignoring coordinated solvents, and the channel is decorated by four regular and four distorted zinc paddlewheels, two EBTC ligands, and four phenyl groups, with an open window of 4.1 Å in length and 3.8 Å in width (the van der Waals radii of the atoms at opposite sites of the cage have been subtracted). It is evident that the slightly bent ethynylene bonds in EBTC ligands have great contribution to the formation of these cages and tunnels. Similarly, **IZE-3** has very large pore volume. Its total solvent-accessible pore volume from single crystal structure is 66.8% calculated from PLATON/SOLV program.[18b]

As for its topology, two kinds of $[Zn_2(CO_2)_4]$ paddlewheels (the regular and the distorted) can be considered as two types of SBUs, and each can be viewed as 4-c node. The two types of 4-c SBUs are connected by EBTC linkers which can be served as two 3-c vertices; thus, a novel (3,4,4)-c **hyx** net[18a] comes into being, with point symbol of $(6.7^2)_4(6^2.8^2.10^2)(7^2.8^2.11^2)$ and vertex symbol of $(6.7.7)_4(7_2.7_2.8.8.12.12)(6.6.8.8.10_2.10_2)$.[19e]

From the above structural description, it is clear that isomers **IZE-1**, **IZE-2**, and **IZE-3** exhibit different frameworks although they are composed of the same component $[Zn_2(EBTC)-(H_2O)_2]$. More specifically, **IZE-1** and **IZE-2** can be considered as orientation isomers[11b] because of the different ligand orientation, while **IZE-3** and **IZE-1**/**IZE-2** can be thought as conformational isomers[11b] since the conformation of ligand EBTC and $[Zn_2(CO_2)_4]$ SBUs are different between them. It is obvious that the reaction medium plays an important role in the construction of such different structural networks, which might be termed as guest- or additive-induced isomerism,[2] though we now do not exactly know how the guest (solvent DMF or DMSO) or the additive (AIP or BPP) affects the

relative isomer precursors including the crystal nucleus and the self-assembled oligomers in the solution and then promote or inhibit the formation of a particular isomer over another. As for the construction of isomers **IZE-1** and **IZE-2** having only one kind of regular $Zn_2(CO_2)_4$ paddlewheel, maybe **IZE-1** is favored for solvent DMF and prefers a higher acidic system (from PXRD; it is sure that **IZE-1** can also be obtained only with DMF as solvent, but its crystal is not so good as that with HNO_3 addition, and DMSO and 5-aminoisophthalic acid (AIP) may be propitious to the formation of **IZE-2**. While for the preparation of **IZE-3** with novel topology, the addition of a small amount of 1,3-bi(4-pyridyl)propane (BPP) leads to two different kinds of $Zn_2(CO_2)_4$ paddlewheels, among which one is severely distorted. In this case, the flexible additive BPP with weak coordinative ability, whose length is comparable to that of ligand EBTC, may be used as template agent during the reaction of EBTC with zinc ions, inducing the linear and relatively rigid EBTC ligand bent and resulting in two different $Zn_2(CO_2)_4$ paddlewheels. Moreover, the size/shape of BPP is compatible with the framework cavities of **IZE-3**, which may further promote its template effect. Furthermore, it should be noted that BPP would coordinate to zinc ions with a little water and DMSO but without nitric acid in the reaction system of **IZE-3**, leading to quite different structural motifs (Figure S5). This further demonstrated that solvent plays an important role in the construction of MOFs.

Moreover, it is remarkable that proper reaction time is also an essential factor for the construction of such paddlewheel networks. Longer reaction time is a disadvantage for the formation of **IZE-1** since under the same reaction condition except for longer reaction time up to 24 h, mixed crystals of **IZE-1** and BAF-2[21] were obtained. It is reported that BAF-2 without paddlewheel structure is synthesized from H_4EBTC with $Zn(NO_3)_2$ using DMF or DEF as solvent at 90 °C for 40 h.[21]

PXRD Patterns and Thermal Stability Analyses. The phase purity of the bulk crystalline samples is independently confirmed by powder X-ray diffraction (PXRD, Figure S6). The PXRD of all the as-synthesized products gives satisfactory XRD patterns which closely match the simulated ones from the single-crystal data, indicating that such microporous MOFs constructed from EBTC and zinc salts are in a pure phase.

The stability of them is determined by thermal gravimetric analysis (TGA, Figure S7). **IZE-1** exhibits 39.3% weight loss from room temperature to 360 °C, which is in agreement with the calculated data (39.8%) of deliberating 2 coordinated H_2O, 5.5 guest H_2O, and 2.5 guest DMF molecules per $[Zn_2(EBTC)]$ unit. With further heating, the skeleton may start to decompose. Similar stability is observed for **IZE-2**. The 39.0% weight loss in the range 25−253 °C corresponds to the 2 coordinated H_2O, 10.5 guest H_2O, 0.5 DMF, and 0.5 DMSO molecules per $[Zn_2(EBTC)]$ unit (calcd: 38.5%). As for **IZE-3**, 30.2% weight loss is observed in the range 25−320 °C, corresponding to the 2 coordinated H_2O, 1.5 guest H_2O, and 2 DMF molecules per $[Zn_2(EBTC)]$ unit (calcd: 30.3%). Following the release of all coordinated water and guest solvents within the MOFs, they all immediately decompose.

Photoluminescent Properties. The solid-state luminescence of the three zinc isomers **IZE-1**, **IZE-2**, and **IZE-3**, as well as the free ligand H_4EBTC, is investigated at room temperature, as depicted in Figure 4. All of them display fluorescent emission bands at about 399, 400, and 427 nm upon excitation at 382, 381, and 351 nm, respectively. These
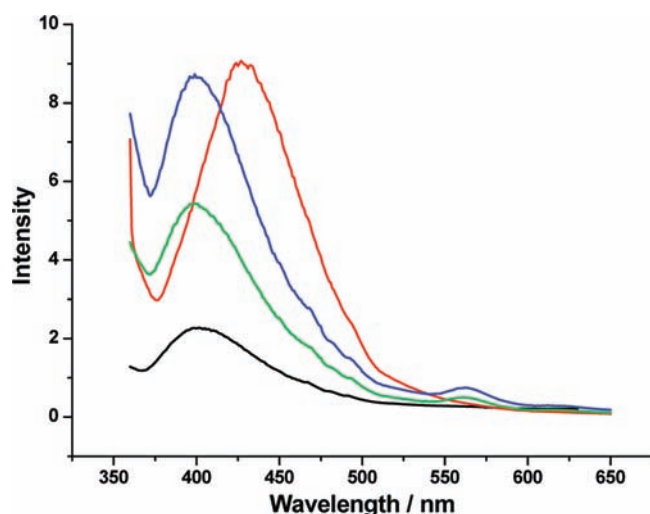
Figure 4. Fluorescent emission spectra of ligand EBTC (black) and complexes **IZE-1** (blue), **IZE-2** (green), **IZE-3** (red) in solid state at room temperature.

bands can probably be assigned to the $\pi-\pi^*$ intraligand fluorescent emission since similar emission is observed at 402 nm upon excitation at 342 nm for their blocking ligand H_4EBTC. Compared with the free ligand, the fluorescence intensity of all these coordination compounds is greatly enhanced, especially for **IZE-1** and **IZE-3**. The enhancement of fluorescence intensity in these complexes is probably due to the unique coordination of the ligand to the Zn^{2+} center, which is increasing the conformational rigidity of the ligand, thereby

reducing the nonradiative decay of the intraligand $(\pi-\pi^*)$ excited state.[22] Furthermore, the emission band of **IZE-3** exhibits a large red shift, while **IZE-1** and **IZE-2** represent a little blue shift upon coordination. This is presumably associated with their different frameworks.

The fluorescence lifetime, τ, of the three isomeric complexes is investigated in the solid state at room temperature, and the curves of the fluorescence decay of them are illustrated in Figure S8. The process of fluorescence decay for them all follows a single exponential decay law, giving luminescence lifetimes of 1.932, 1.769, and 2.032 ms, respectively, significantly longer than those reported for other fluorescent zinc complexes and MOFs which are often on the nanosecond time scale,[23] indicating highly rigidified in the solid matrices.[23e,24] Due to their remarkable luminescence, they appear to be good candidates of novel hybrid inorganic–organic optic materials.

Quantum Chemical Studies on Relative Stabilities of Isomers. The relative thermodynamic stabilities of **IZE-1**, **IZE-2**, and **IZE-3** were investigated through quantum chemical calculations of these systems on the basis of experimental crystal structures. Cluster models, containing 8 five-coordinated Zn^{2+} and related coordination environments for different crystals, were adopted as shown in Figure 5. We performed single-point calculations of cluster models by employing the hybrid density functional theory (DFT) with the B3LYP exchange-correlation functional[25,26] and LANL2DZ[27] basis sets. All calculations were carried out by using the Gaussian 09 program.[28]
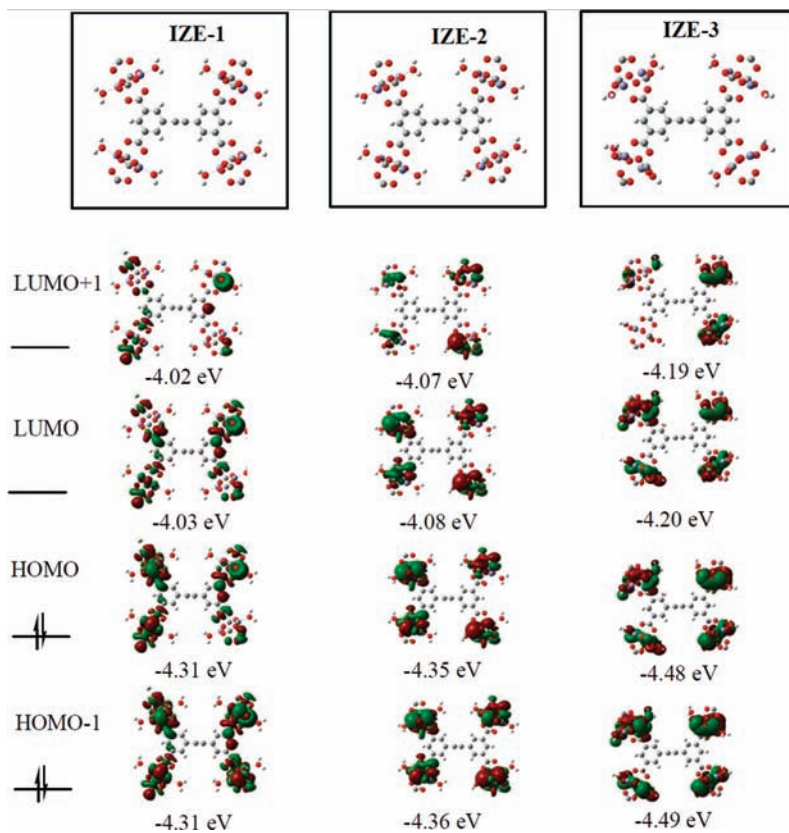

Figure 5. Cluster models and frontier molecular orbitals as well as their orbital energies calculated at B3LYP/LANL2DZ level for **IZE-1**, **IZE-2**, and **IZE-3**.

DFT ground state energies and HOMO−LUMO gaps for three different cluster models are listed in Table 2. It is shown

Table 2. Comparison of the Ground State Energies and HOMO−LUMO Gaps for Three Different Cluster Models Calculated at B3LYP/LANL2DZ Level

	IZE-1	IZE-2	IZE-3
relative ground state energy [kcal/mol]	58.8	55.7	0.0
HOMO−LUMO gap [kcal/mol]	6.47	6.27	6.38

that both the total energies and HOMO−LUMO gap values are very close for all three different cluster models. The similarity of their thermodynamic stabilities is also demonstrated from their very similar frontier molecular orbitals illustrated in Figure 5. The two highest occupied MOs (HOMO − 1 and HOMO) are nearly degenerate while the two lowest unoccupied MOs (LUMO and LUMO + 1) are also nearly degenerate, and all the four frontier MOs are dominated by the localized metal−ligand d−π bonding interactions. From these thermodynamic data, it is understandable that all the 3 isomers could be stable under certain conditions, but a minor altered external factor may lead them to some other different structures.

Quantum Chemical Studies on the Interactions between Solvent Molecules and Isomers. In spite of already being shown to have very close thermodynamic stabilities, **IZE-1**, **IZE-2**, and **IZE-3** have been experimentally determined to present quite different binding properties under different solvent environments. In order to provide insight into the solvent effects for **IZE-1**, **IZE-2**, and **IZE-3**, we performed semiempirical quantum chemical calculations for the interactions between them and solvent molecules at PM3 level.[29] All calculations were carried out by using the Gaussian 09 program.[28]
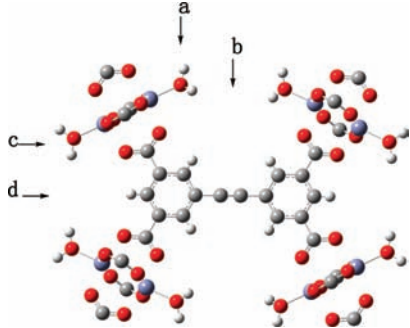
Considering the symmetry of the cluster models, we may specify four types of binding positions for DMF or DMSO solvent molecules, as illustrated in Table 3. The calculated binding energy values for DMF and DMSO binding to **IZE-1**, **IZE-2**, and **IZE-3** at the above four type binding positions are listed in Table 3. It is clearly shown that most binding energies

for possible binding patterns are around 2−10 kcal/mol, which are in the typical energy range of hydrogen bonding. This fact implies that the main interactions between DMF or DMSO solvent molecules and **IZE-1**, **IZE-2**, and **IZE-3** may be hydrogen bonding, which is further verified through our geometry analysis where we found the distances between the oxygen atoms in DMF or DMSO molecules and the hydrogen atoms in H_2O molecules coordinating Zn^{2+} are around 1.80 Å, the typical length of hydrogen bonding. Comparing **IZE-1** with **IZE-3**, DMF binding energies in the former case are obviously much larger than those in the latter case, indicating that more DMF molecules can be bound to the cluster model of **IZE-1** than that of **IZE-3**. Optimized geometries for cluster models under DMF and/or DMSO solvent environments are shown in Figure 6, where stable **IZE-1** structure binding 10 DMF molecules and stable **IZE-3** structure binding 8 DMF molecules are presented, in good agreement with experimental observations. As for the case of **IZE-2**, DMSO has largest binding energy at the position of *a* and consequently the most possible DMF binding position is *c* although DMF has a larger binding energy value at the position of *b* (locating DMF at neighboring binding positions very close to that of DMSO is energetically unfavorable due to the geometrical constraints). The optimized geometry for the composite system of the cluster model of **IZE-2** binding 2 DMF molecules and 2 DMSO molecules is also shown in Figure 6. It could be found from the figure that there are still many positions unbound which may be provided to many small solvent molecules like H_2O, which is consistent with the experimental observations.

CONCLUSIONS

In summary, by elaborate controlling the reaction conditions of zinc salts with the rectangular tetracarboxylate EBTC ligand, three porous supramolecular isomers could be successfully obtained, in which **IZE-3** exhibits the unusual (3,4,4)-c hyx net with an unprecedented $(6.7^2)_4(6^2.8^2.10^2)(7^2.8^2.11^2)$ topology. These three isomers exhibit great solid-state luminescence properties and relatively long lifetimes on the microsecond time scale. Theoretical studies indicate that the three isomers have similar thermodynamic stabilities, further verifying that all of

Table 3. Binding Energies of DMF and DMSO at Different Binding Positions for Three Different Cluster Models Calculated at Semiempirical PM3 Level[a]

complex	binding energy (DMF) [kcal/mol]				binding energy (DMSO) [kcal/mol]			
	a	b	c	d	a	b	c	d
IZE-1	6.93	−	6.68	5.11	11.16	−	9.99	8.66
IZE-2	3.48	7.47	4.98	3.47	11.34	9.04	10.04	10.22
IZE-3	4.04	1.20	2.58	−	7.97	7.60	7.74	−

[a]Due to the geometrical constraints, some binding patterns are energetically unfavorable, and therefore, the values are shown as "−".
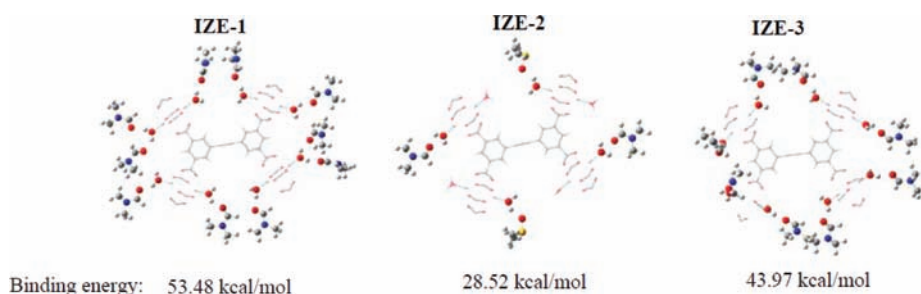
Figure 6. Optimized geometries and calculated total binding energies for the cluster models of **IZE-1**, **IZE-2**, and **IZE-3** binding DMF and/or DMSO solvent molecules through semiempirical PM3 calculations.

them can stably exist in some case and a tiny alterative external factor could vary them in different structures. This work will contribute to the further development of our knowledge on supramolecular chemistry and crystal engineering concerning MOFs.

■ ASSOCIATED CONTENT

ⓢ Supporting Information

Crystal photographs, crystal structures and topologies, PXRD patterns, TG analysis, crystallographic data and cif files of **IZE-1**, **IZE-2**, and **IZE-3**. This material is available free of charge via the Internet at http://pubs.acs.org.

■ AUTHOR INFORMATION

Corresponding Author
*E-mail: wwzhang@nju.edu.cn (W.-W.Z.), bjunfeng@nju.edu. cn (J.B.).

Notes
The authors declare no competing financial interest.

■ ACKNOWLEDGMENTS

■ REFERENCES

(1) (a) Zaworotko, M. J. *Nat. Chem.* **2009**, *1*, 267−268. (b) Zaworotko, M. J. *Nature* **2008**, *451*, 410−411. (c) Ma, S.; Sun, D.; Yuan, D.; Wang, X. S.; Zhou, H. C. *J. Am. Chem. Soc.* **2009**, *131*, 6445−6451. (d) Férey, G.; Mellot-Draznieks, C.; Serre, C.; Millange, F.; Dutour, J.; Surblé, S.; Margiolaki, I. *Science* **2005**, *309*, 2040−2042. (e) Zhang, J.-P.; Chen, X.-M. *J. Am. Chem. Soc.* **2008**, *130*, 6010−6017.
(2) Zhang, J.-P.; Huang, X.-C.; Chen, X.-M. *Chem. Soc. Rev.* **2009**, *38*, 2385−2396.
(3) (a) Kawano, M.; Kawamichi, T.; Haneda, T.; Kojima, T.; Fujita, M. *J. Am. Chem. Soc.* **2007**, *129*, 15418−15419. (b) Wang, Y. T.; Fan, H. H.; Wang, H. Z.; Chen, X. M. *Inorg. Chem.* **2005**, *44*, 4148−4150.
(4) Carlucci, L.; Ciani, G.; Proserpio, D. M.; Rizzato, S. *New J. Chem.* **2003**, *27*, 483−489.
(5) Shin, D. M.; Lee, I. S.; Cho, D.; Chung, Y. K. *Inorg. Chem.* **2003**, *42*, 7722−7724.
(6) (a) Zheng, B.; Dong, H.; Bai, J.; Li, Y.; Li, S.; Scheer, M. *J. Am. Chem. Soc.* **2007**, *129*, 7778−7779. (b) Mahata, P.; Sundaresan, A.; Natarajan, S. *Chem. Commun.* **2007**, 4471−4473. (c) Zhang, J. J.; Wojtas, L.; Larsen, R. W.; Eddaoudi, M.; Zaworotko, M. J. *J. Am. Chem. Soc.* **2009**, *131*, 17040−17041.
(7) (a) Lee, I. S.; MokShin, D.; Chung, Y. K. *Chem.—Eur. J.* **2004**, *10*, 3158−3165. (b) Long, D.-L.; Blake, A. J.; Champness, N. R.; Wilson, C.; Schröder, M. *Chem.—Eur. J.* **2002**, *8*, 2026−2033. (c) Blake, A. J.; Champness, N. R.; Cooke, P. A.; Nicolson, J. E. B. *Chem. Commun.* **2000**, 665−666.
(8) Wu, S. T.; Long, L. S.; Huang, R. B.; Zheng, L. S. *Cryst. Growth Des.* **2007**, *7*, 1746−1752.
(9) Lu, X. Q.; Jiang, J. J.; Chen, C. L.; Kang, B. S.; Su, C. Y. *Inorg. Chem.* **2005**, *44*, 4515−4521.
(10) (a) Muthu, S.; Yip, J. H. K.; Vittal, J. J. *J. Chem. Soc., Dalton Trans.* **2001**, 3577−3584. (b) Barnett, S. A.; Blake, A. J.; Champness, N. R.; Wilson, C. *Chem. Commun.* **2002**, 1640−1641. (c) Oh, M.; Carpenter, G. B.; Sweigart, D. A. *Angew. Chem., Int. Ed.* **2002**, *41*, 3650−3653. (d) Shin, D. M.; Lee, I. S.; Chung, Y. K.; Lah, M. S. *Chem. Commun.* **2003**, 1036−1037. (e) Yang, X.-D.; Ranford, J. D.; Vittal, J. J. *Cryst. Growth Des.* **2004**, *4*, 781−788. (f) Horikoshi, R.; Mochida, T.; Kurihara, M.; Mikuriya, M. *Cryst. Growth Des.* **2005**, *5*, 243−249. (g) Fromm, K. M.; Doimeadios, J. L. S.; Robin, A. Y. *Chem. Commun.* **2005**, 4548−4550. (h) Zhan, S.-Z.; Li, D.; Zhou, X.-P.; Zhou, X.-H. *Inorg. Chem.* **2006**, *45*, 9163−9165. (i) Ma, S.; Sun, D.; Ambrogio, M.; Fillinger, J. A.; Parkin, S.; Zhou, H. C. *J. Am. Chem. Soc.* **2007**, *129*, 1858−1859. (j) Hao, Z.-M.; Zhang, X.-M. *Cryst. Growth Des.* **2007**, *7*, 64−68. (k) Wang, C.-C.; Lin, W.-Z.; Huang, W.-T.; Koa, M.-J.; Lee, G.-H.; Ho, M.-L.; Lin, C.-W.; Shih, C.-W.; Chou, P.-T. *Chem. Commun.* **2008**, 1299−1301. (l) Ma, L.; Lin, W. *J. Am. Chem. Soc.* **2008**, *130*, 13834−13835. (m) Sun, D.; Ma, S.; Simmons, J. M.; Li, J. R.; Yuan, D.; Zhou, H. C. *Chem. Commun.* **2010**, *46*, 1329−1331.
(11) (a) Moulton, B.; Zaworotko, M. J. *Chem. Rev.* **2001**, *101*, 1629−1658. (b) Makal, T. A.; Yakovenko, A. A.; Zhou, H.-C. *J. Phys. Chem. Lett.* **2011**, *2*, 1682−1689.
(12) (a) Bourne, S. A.; Lu, J.; Mondal, A.; Moulton, B.; Zaworotko, M. J. *Angew. Chem., Int. Ed.* **2001**, *40*, 2111−2113. (b) Furukawa, H.; Kim, J.; Ockwig, N. W.; O'Keeffe, M.; Yaghi, O. M. *J. Am. Chem. Soc.* **2008**, *130*, 11650−11661. (c) Burrows, A. D.; Frost, C. G.; Mahon, M. F.; Winsper, M.; Richardson, C.; Attfield, J. P.; Rodgers, J. A. *Dalton Trans.* **2008**, *47*, 6788−6795. (d) Ma, S.; Sun, D.; Simmons, J. M.; Collier, C. D.; Yuan, D.; Zhou, H. C. *J. Am. Chem. Soc.* **2008**, *130*, 1012−1016.
(13) (a) Chui, S. S. Y.; Lo, S. M. F.; Charmant, J. P. H.; Orpen, A. G.; Williams, I. D. *Science* **1999**, *283*, 1148−1150. (b) Sun, D.; Ma, S.; Ke, Y.; Collins, D. J.; Zhou, H. C. *J. Am. Chem. Soc.* **2006**, *128*, 3896−3897. (c) Ma, S.; Zhou, H. C. *J. Am. Chem. Soc.* **2006**, *128*, 11734−11735. (d) Yan, Y.; Lin, X.; Yang, S.; Blake, A. J.; Dailly, A.; Champness, N. R.; Hubberstey, P.; Schröder, M. *Chem. Commun.* **2009**, *9*, 1025−1027. (e) Zhao, X.; He, H.; Hu, T.; Dai, F.; Sun, D. *Inorg. Chem.* **2009**, *48*, 8057−8059.
(14) (a) Chen, B.; Ockwig, N. W.; Millward, A. R.; Contreras, D. S.; Yaghi, O. M. *Angew. Chem., Int. Ed.* **2005**, *44*, 4745−4749. (b) Lin, X.; Jia, J.; Zhao, X.; Thomas, K. M.; Blake, A. J.; Walker, G. S.;

Champness, N. R.; Hubberstey, P.; Schröder, M. *Angew. Chem., Int. Ed.* **2006**, *45*, 7358−7364. (c) Ma, L.; Lee, J. Y.; Li, J.; Lin, W. *Inorg. Chem.* **2008**, *47*, 3955−3957. (d) Wang, X. S.; Ma, S.; Rauch, K.; Simmons, J. M.; Yuan, D.; Wang, X.; Yildirim, T.; Cole, W. C.; López, J. J.; de Meijere, A.; Zhou, H. C. *Chem. Mater.* **2008**, *20*, 3145−3152. (e) Wu, J. Y.; Yang, S. L.; Luo, T. T.; Liu, Y. H.; Cheng, Y. W.; Chen, Y. F.; Wen, Y. S.; Lin, L. G.; Lu, K. L. *Chem.—Eur. J* **2008**, *14*, 7136−7139. (f) Lin, X.; Telepeni, I.; Blake, A. J.; Dailly, A.; Brown, C. M.; Simmons, J. M.; Zoppi, M.; Walker, G. S.; Thomas, K. M.; Mays, T. J.; Hubberstey, P.; Champness, N. R.; Schröder, M. *J. Am. Chem. Soc.* **2009**, *131*, 2159−2171. (g) Wu, S.; Ma, L.; Long, L. S.; Zheng, L. S.; Lin, W. *Inorg. Chem.* **2009**, *48*, 2436−2442. (h) Wu, J. Y.; Ding, M. T.; Wen, Y. S.; Liu, Y. H.; Lu, K. L. *Chem.—Eur. J.* **2009**, *15*, 3604−3614. (i) Zhao, D.; Yuan, D.; Yakovenko, A.; Zhou, H.-C. *Chem. Commun.* **2010**, *46*, 4196−4198.

(15) (a) Zou, Y.; Park, M.; Hong, S.; Lah, M. S. *Chem. Commun.* **2008**, *20*, 2340−2342. (b) Yan, Y.; Telepeni, I.; Yang, S.; Lin, X.; Kockelmann, W.; Daily, A.; Blake, A. J.; Lewis, W.; Walker, G. S.; Allan, D. R.; Barnett, S. A.; Champness, N. R.; Schröder, M. *J. Am. Chem. Soc.* **2010**, *132*, 4092−4094.

(16) Hu, Y. X.; Xiang, S. C.; Zhang, W. W.; Zhang, Z. X.; Wang, L.; Bai, J. F.; Chen, B. L. *Chem. Commun.* **2009**, *48*, 7551−7553.

(17) (a) Thorand, S.; Krause, N. *J. Org. Chem.* **1998**, *63*, 8551−8553. (b) Sonogashira, K. *J. Organomet. Chem.* **2002**, *653*, 46−49. (c) Bodwell, G. J.; Miller, D. O.; Vermeij, R. J. *Org. Lett.* **2001**, *3*, 2093−2096. (d) Li, C. Z.; Zhu, J.; Wu, Z. Q.; Hou, J. L.; Li, C.; Shao, X. B.; Jiang, X. K.; Li, Z. T.; Gao, X.; Wang, Q. R. *Tetrahedron* **2006**, *62*, 6973−6980.

(18) (a) Blatov, V. A. *CompComm Newsletter* **2006**, *7*, 4−38. (b) Spek, A. L. *J. Appl. Crystallogr.* **2003**, *36*, 7−13. (c) Sluis, P. V. D.; Spek, A. L. *Acta Crystallogr., Sect. A* **1990**, *46*, 194−201.

(19) (a) O'Keeffe, M.; Yaghi, O. M. *Chem. Rev.* **2012**, *112*, 675−702. (b) Alexandrov, E. V.; Blatov, V. A.; Kochetkov, A. V.; Proserpio, D. M. *CrystEngComm* **2011**, *13*, 3947−3958. (c) O'Keeffe, M.; Peskov, M. A.; Ramsden, S. J.; Yaghi, O. M. *Acc. Chem. Res.* **2008**, *41*, 1782−1789. (d) Ramsden, S. J.; Robins, V.; Hyde, S. T. *Acta Crystallogr., Sect. A* **2009**, *65*, 81−108. (e) Blatov, V. A.; O'Keeffe, M.; Proserpio, D. M. *CrystEngComm* **2010**, *12*, 44−48.

(20) Xue, M.; Zhu, G.; Li, Y.; Zhao, X.; Jin, Z.; Kang, E.; Qiu, S. *Cryst. Growth Des.* **2008**, *8*, 2478−2483.

(21) Hausdorf, S.; Seichter, W.; Weber, E.; Mertens, F. O. R. L. *Dalton Trans.* **2009**, *7*, 1107−1113.

(22) Kurtz, S. K.; Perry, T. T. *J. Appl. Phys.* **1968**, *39*, 3798−3813.

(23) (a) Chen, Z.-F.; Xiong, R.-G.; Zhang, J.; Chen, X.-T.; Xue, Z.-L.; You, X.-Z. *Inorg. Chem.* **2001**, *40*, 4075−4077. (b) Mizukami, S.; Houjou, H.; Sugaya, K.; Koyama, E.; Tokuhisa, H.; Sasaki, T.; Kanesato, M. *Chem. Mater.* **2005**, *17*, 50−56. (c) De la Escosura, A.; Marténez-Déaz, M. V.; Guldi, D. M.; Torres, T. *J. Am. Chem. Soc.* **2006**, *128*, 4112−4118. (d) Hajjaj, F.; Yoon, Z. S.; Yoon, M.-C.; Park, J.; Satake, A.; Kim, D.; Kobuke, Y. *J. Am. Chem. Soc.* **2006**, *128*, 4612−4623. (e) Bauer, C. A.; Timofeeva, T. V.; Settersten, T. B.; Patterson, B. D.; Liu, V. H.; Simmons, B. A.; Allendorf, M. D. *J. Am. Chem. Soc.* **2007**, *129*, 7136−7144. (f) Girardot, C.; Lemercier, G.; Mulatier, J.-C.; Chauvin, J.; Baldeck, P. L.; Andraud, C. *Dalton Trans.* **2007**, 3421−3426. (g) Liu, Q.-Y.; Wang, Y.-L.; Du, Z.-Y.; Shan, Z.-M.; Yang, E.-L.; Zhang, N. *Aust. J. Chem.* **2010**, *63*, 1565−1572. (h) Roy, A. S.; Saha, P.; Mitra, P.; Maity, S. S.; Ghosh, S.; Ghosh, P. *Dalton Trans.* **2011**, *40*, 7375−7384.

(24) Pyun, C.-H.; Lyle, T. A.; Daub, G. H.; Park, M. *Chem. Phys. Lett.* **1986**, *124*, 48−52.

(25) Becke, A. D. *J. Chem. Phys.* **1993**, *98*, 5648−5652.

(26) Lee, C.; Yang, W.; Parr, R. G. *Phys. Rev. B* **1988**, *37*, 785−789.

(27) Hay, P. J.; Wadt, W. R. *J. Chem. Phys.* **1985**, *82*, 299−310.

(28) Frisch, M. J.; Trucks, G. W.; Schlegel, H. B.; Scuseria, G. E.; Robb, M. A.; Cheeseman, J. R.; Scalmani, G.; Barone, V.; Mennucci, B.; Petersson, G. A.; Nakatsuji, H.; Caricato, M.; Li, X.; Hratchian, H. P.; Izmaylov, A. F.; Bloino, J.; Zheng, G.; Sonnenberg, J. L.; Hada, M.; Ehara, M.; Toyota, K.; Fukuda, R.; Hasegawa, J.; Ishida, M.; Nakajima, T.; Honda, Y.; Kitao, O.; Nakai, H.; Vreven, T.; Montgomery, J. A., Jr.; Peralta, J. E.; Ogliaro, F.; Bearpark, M.; Heyd, J. J.; Brothers, E.; Kudin, K. N.; Staroverov, V. N.; Kobayashi, R.; Normand, J.; Raghavachari, K.; Rendell, A.; Burant, J. C.; Iyengar, S. S.; Tomasi, J.; Cossi, M.; Rega, N.; Millam, J. M.; Klene, M.; Knox, J. E.; Cross, J. B.; Bakken, V.; Adamo, C.; Jaramillo, J.; Gomperts, R.; Stratmann, R. E.; Yazyev, O.; Austin, A. J.; Cammi, R.; Pomelli, C.; Ochterski, J. W.; Martin, R. L.; Morokuma, K.; Zakrzewski, V. G.; Voth, G. A.; Salvador, P.; Dannenberg, J. J.; Dapprich, S.; Daniels, A. D.; Ö. Farkas, Foresman, J. B.; Ortiz, J. V.; Cioslowski, J.; , Fox, D. J. *Gaussian 09, Revision A.1*; Gaussian, Inc.: Wallingford, CT, 2009.

(29) Stewart, J. J. P. *J. Comput. Chem.* **1989**, *10*, 209−220.